

A Series of Transition-metal Coordination Complexes Assembled from 3-Nitrophthalic Acid and Thiabendazole: Synthesis, Structure and Properties

Wen-Jia Xu, Qi-Jun Xue,[†] Peng Liang, Ling-Yu Zhang, Yan-Feng Huang, and Yu Feng*

College of Chemistry and Chemical Engineering, Guangxi University for Nationalities, Nanning 530006, P.R. China

**E-mail: fengyu19871212@126.com*

[†]College of pharmacy, Liaoning University, Shenyang 110036, P.R. China

Received September 3, 2013, Accepted October 28, 2013

In order to explore new coordination frameworks with novel designed 3-nitrophthalic acid and the same N-donor ancillary ligand, a series of novel coordination complexes, namely, $[\text{Cd}_2(3\text{-NPA})_2(\text{TBZ})_2(\text{H}_2\text{O})_2] \cdot 2\text{H}_2\text{O}$ (**1**), $[\text{Zn}_2(3\text{-NPA})_2(\text{TBZ})_2]$ (**2**), $[\text{Zn}_2\text{O}(3\text{-NPA})(\text{TBZ})(\text{H}_2\text{O})]_n$ (**3**), $[\text{Co}(3\text{-NPA})(\text{TBZ})(\text{H}_2\text{O})]_n$ (**4**) (3-NPAH₂ = 3-nitrophthalic acid), have been hydrothermally synthesized through the reaction of 3-nitrophthalic acid with divalent transition-metal salts in the presence of N-donor ancillary coligand (TBZ = thiabendazole). As a result of various coordination modes of the versatile 3-NPAH₂ and the coligand TBZ, these complexes exhibit structural diversity. X-ray structure analysis reveals that **1** and **2** are 0D molecular rings, while **3** and **4** are one-dimensional (1D) infinite chain polymers. And the weak O–H···O hydrogen bonds and C–H···O nonclassical hydrogen bonds as well as π - π stacking also play important roles in affecting the final structure where complexes **1**, **3** and **4** have 3D supramolecular architectures, while complex **2** has a 2D supramolecular network. Also, IR spectra, fluorescence properties and thermal decomposition process of complexes **1-4** were investigated.

Key Words : Transition-metal complexes, Coordination modes of the carboxylate groups, 3-Nitrophthalic acid, Thiabendazole

Introduction

The design and synthesis of zero-, one-, two-, or three-dimensional (0D, 1D, 2D, or 3D) coordination assemblies by utilizing directional metalligand dative bonds has attracted considerable interest in recent years, which may bring both intriguing architectures and tailor-made applications in such fields as porosity, magnetics, optoelectronics, catalysis, and so on.^{1,2} As it is known, it is still a big challenge to predict the final structures of desired crystalline products, since the self-assembly process of crystalline products is influenced by many factors, such as metal ions, organic ligands, counter ions, solvent system, temperature and pH of reaction system.³⁻⁵ The delicate balance between the adaptability of the organic ligands with the plentiful and versatile coordination modes of the central metals as well as the coparticipation of counteranions and solvent molecules leads to the formation of either discrete polynuclear complexes or infinite coordination polymers, affording great opportunities for the construction of novel and unusual metalorganic crystalline materials.^{6,7} In order to obtain new coordination complexes with various topological structures, multicarboxylates are often selected as bridging ligands to construct coordination complexes not only due to their versatile coordination modes to metal centers but also their strong ability to act as hydrogen bonding acceptors and donors.⁸⁻¹¹ Especially, the 3-nitrophthalic acid can serve as excellent candidates for building highly connected or catenulate coordination frameworks due to their versatile bridging fashions.^{12,13}

Apart from the carboxylate linkers, N-donor ligands are frequently used as ancillary ligands to give multipodal anions acting as bridging, chelating, and charge balance ligands for synthesizing polynuclear species.¹⁴ Moreover, the hybrid coordination complexes constructed by thiabendazole and 3-nitrophthalic acid are rarely documented to date. With this understanding, 3-NPAH₂ (3-nitrophthalic acid) was chosen as the organic ligand, TBZ (thiabendazole) was chosen as neutral co-ligand to construct new transition-metal coordination complexes under the hydrothermal reaction. This paper presents the syntheses, structures, luminescent properties and thermal stabilities of four novel coordination complexes $[\text{Cd}_2(3\text{-NPA})_2(\text{TBZ})_2(\text{H}_2\text{O})_2] \cdot 2\text{H}_2\text{O}$ (**1**), $[\text{Zn}_2(3\text{-NPA})_2(\text{TBZ})_2]$ (**2**), $[\text{Zn}_2\text{O}(3\text{-NPA})(\text{TBZ})(\text{H}_2\text{O})]_n$ (**3**), and $[\text{Co}(3\text{-NPA})(\text{TBZ})(\text{H}_2\text{O})]_n$ (**4**).

Experimental

All chemicals were commercial materials of analytical grade and used without purification. Elemental analysis for C, H, N and S was carried out on a Perkin-Elmer 2400 II elemental analyzer. The FT-IR spectrum was obtained on a PE Spectrum One FT-IR Spectrometer Fourier transform infrared spectroscopy in the 4000-400 cm⁻¹ regions, using KBr pellets. Perkin-Elmer Diamond TG/DTA thermal analyzer was used to record simultaneous TG and DTG curves in the static air atmosphere at a heating rate of 10 K min⁻¹ in the temperature range 25-1000 °C using platinum crucibles. Fluorescence spectra were recorded with F-2500 FL Spectro-

photometer analyzer.

Synthesis of the Complex $[\text{Cd}_2(\text{3-NPA})_2(\text{TBZ})_2(\text{H}_2\text{O})_2] \cdot 2\text{H}_2\text{O}$ (1): A mixture of $\text{Cd}(\text{NO}_3)_2 \cdot 4\text{H}_2\text{O}$ (0.309 g, 1.00 mmol), 3-NPAH₂ (0.106 g, 0.500 mmol), and TBZ (0.101 g, 0.500 mmol) was added to 9 mL mixed solvent of DMF/H₂O (volume ratio 1:3), and its pH was controlled in the rang 5-6 with a 0.4 mol·L⁻¹ aqueous solution of potassium hydroxide. After the mixture was stirred for 30 min, it was placed in a 30 mL Teflon-lined stainless reactor and heated at 145 °C for 3 days and then slowly cooled to room temperature at a rate of 5 °C per hour. The block crystals suitable for X-ray diffraction were isolated directly (Yield: 60%, based on Cd). Anal. Calcd for C₃₆H₂₆Cd₂N₈O₁₆S₂ (%): C, 38.76; H, 2.35; N, 10.04; S, 5.75. Found: C, 38.75; H, 2.38; N, 10.03; S, 5.73. IR data (KBr pellets, cm⁻¹): 3447 (s), 3105 (m), 1652 (s), 1587 (s), 1556 (s), 1539 (m), 1520 (m), 1507 (m), 1457 (m), 1396 (m), 1354 (s), 1327 (m), 1012 (m), 921 (w), 877 (m), 837 (w), 746 (w), 667 (w).

Synthesis of Complex $[\text{Zn}_2(\text{3-NPA})_2(\text{TBZ})_2]$ (2): The same synthetic procedure as that for **1** was used except that $\text{Cd}(\text{NO}_3)_2 \cdot 4\text{H}_2\text{O}$ (0.309 g, 1.00 mmol) was replaced by ZnCl_2 (0.136 g, 1.00 mmol). The block crystals of **2** were obtained in 65% yield based on Zn. Anal. Calcd for C₃₆H₁₈N₈O₁₂S₂Zn₂ (%): C, 45.54; H, 1.19; N, 11.80; S, 6.75. Found: C, 45.52; H, 1.18; N, 11.82; S, 6.76. IR data (KBr pellets, cm⁻¹): 1641 (s), 1601 (s), 1557 (s), 1542 (s), 1454 (s), 1415 (s), 1373 (m), 1334 (m), 1014 (m), 925 (w), 832 (w), 751 (w), 708 (w), 664 (w).

Synthesis of Complex $[\text{Zn}_2\text{O}(\text{3-NPA})(\text{TBZ})(\text{H}_2\text{O})_n]$ (3): A solution of 3-NPAH₂ (0.106 g, 0.500 mmol) in 3 mL DMF was added dropwise with stirring at room temperature to a solution of ZnCl_2 (0.136 g, 1.00 mmol) in the mixture of 10 mL water and 5 mL ethanol. Then an aqueous solution of sodium hydroxide was added dropwise with stirring to adjust the pH value of the solution being 6. The resulting mixture was sealed in a 30 mL Teflon-lined stainless reactor, kept under autogenous pressure at 150 °C for 3 days, and then slowly cooled to room temperature at a rate of 5 °C per hour. The block crystals suitable for X-ray diffraction were isolated directly, washed with ethanol and dried in air (Yield: 60%, based on Zn). Anal. Calcd for C₁₈H₁₁N₄O₈SZn₂ (%): C, 37.66; H, 1.93; N, 9.76; S, 5.59. Found: C, 37.65; H, 1.94; N, 9.77; S, 5.57. IR data (KBr pellets, cm⁻¹): 3439 (vs), 1650 (s), 1634 (s), 1557 (s), 1540 (s), 1521 (m), 1507 (s), 1457 (s), 1394 (m), 1338 (m), 1294 (m), 1113 (m), 924 (w), 738 (w), 665 (w).

Synthesis of Complex $[\text{Co}_2(\text{3-NPA})(\text{TBZ})(\text{H}_2\text{O})_n]$ (4): The same synthetic procedure as that for **3** was used except that ZnCl_2 (0.136 g, 1.00 mmol) was replaced by CoCl_2 (0.129 g, 1.00 mmol). The block crystals of **4** were obtained in 65% yield based on Co. Anal. Calcd for C₃₆H₂₂Co₂N₈O₁₄S₂ (%): C, 44.46; H, 2.28; N, 11.52; S, 6.59. Found: C, 44.47; H, 2.27; N, 11.51; S, 6.60. IR data (KBr pellets, cm⁻¹): 3244 (s), 3048 (m), 1557 (s), 1540 (s), 1526 (s), 1506 (m), 1456 (m), 1385 (m), 1376 (s), 1339 (m), 1015 (w), 998 (w), 930 (w), 863 (w), 789 (w), 744 (w), 618 (w).

Crystal Structure Determination. Suitable single crystal

with approximate dimensions were mounted on a glass fiber and used for X-ray diffraction analyses. Data were collected at 293(2) K on a Bruker Apex CCD diffractometer using the ω scan technique with Mo K α radiation ($\lambda = 0.71069 \text{ \AA}$). Absorption corrections were applied using the multi-scan technique.¹⁵ Structures were solved by the Direct Method and refined by full-matrix least-square techniques on F² using SHELXL-97.¹⁶ All non-hydrogen atoms were refined anisotropically. The crystal data and structure refinement details for four complexes are shown in Table S1. Selected bond lengths and angles of the complexes are listed in Table S2, and possible hydrogen bond geometries are given in Table S3.

Crystallographic data for the structures reported here have been deposited with CCDC (Deposition No. CCDC-951514 (1), No. CCDC-951515 (2), No. CCDC-951516 (3), CCDC-951517(4)). These data can be obtained free of charge *via* <http://www.ccdc.cam.ac.uk/conts/retrieving.html> or from CCDC, 12 Union Road, Cambridge CB2 1EZ, UK, E-mail: deposit@ccdc.cam.ac.uk.

Results and Discussion

Description of the Structure. The single-crystal X-ray diffraction analysis reveals that complexes **1**, **2**, and **3** crystallize in the triclinic *P*-1 space group, **4** belongs to the monoclinic system with space group *P*2(1)/*c*.

The asymmetric unit of **1** consists of one Cd(II) ion, one 3-NPA²⁻, one TBZ, one coordinated water molecule and one lattice water molecule. As depicted in Figure 1, there are two deprotonated 3-nitrophthalic acid coordinated by two neighboring Cd(II) cations on the symmetrical position, forming a 14-membered ring, and two carboxylate groups of 3-NPA²⁻ ligand adopt different coordination modes: one carboxylate group adopts $\mu_1\text{-}\eta^1\text{:}\eta^0$ mode and the other adopts $\mu_1\text{-}\eta^1\text{:}\zeta^1$ mode (Figure S1a). The Cd1 is six coordinated by three carboxylate oxygen atoms from two 3-NPA²⁻ ligands and two nitrogen atoms from one TBZ as well as one oxygen atom from one coordinated water molecule to form distorted octahedral geometry. The atoms (N2, O7) occupy the axial

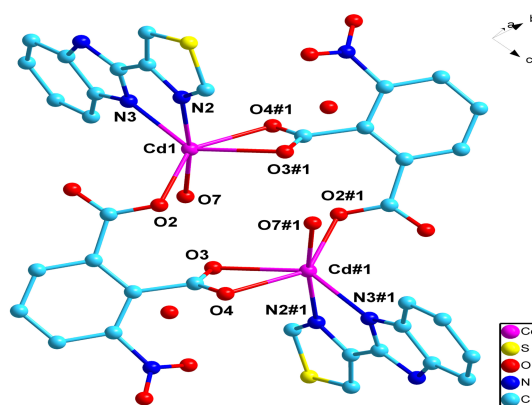


Figure 1. The coordination environment of Cd(II) ion of the complex **1**. All the hydrogen atoms are omitted for clarity. Symmetry codes: #1 = -x, 1-y, 1-z.

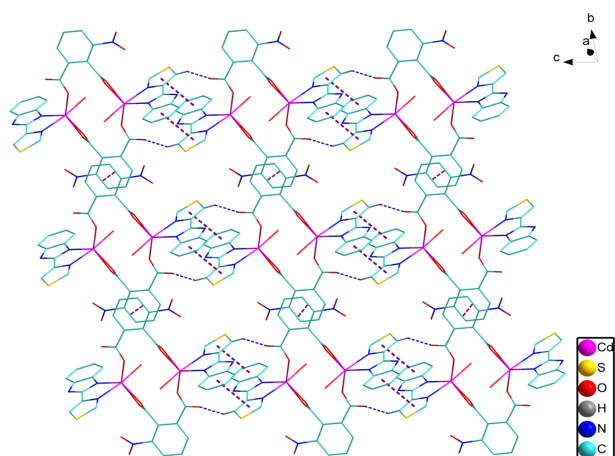


Figure 2. The 2D layered network of complex **1** via H-bonding and π - π stacking interactions. Unnecessary atoms are omitted for clarity.

positions, and the nitrogen atom (N3) and oxygen atoms (O2, O3#1 and O4#1) comprise the equatorial plane. The distances of O and Cd range from 2.261(2) to 2.468(3) Å and the Cd–N bond lengths are 2.270(3) and 2.359(3) Å, which falls in the usual range for similar Cd complexes.¹⁷ The crystal structure is further connected through face-to-face π - π stacking between two adjacent TBZ. Two adjacent TBZ and two adjacent 3-NPA²⁻ molecules are completely parallel with a interplanar separation of *ca.* 3.623(3) and 3.672(3) Å, respectively. The molecules stack with each other via perfect face-to-face π - π interaction and C–H \cdots O hydrogen bonds in arrays to form a 2D supramolecular structure (Figure 2). Moreover, the resulting 2D structure is cross-linked by the weak hydrogen-bond interactions between O–H groups from lattice waters and carboxylate oxygen atoms, thus leading to the formation of a 3D supramolecular architecture (Figure 3). The dimensionality is increased by the very weak C–H \cdots O hydrogen bonds.

There is an obvious difference of the coordination modes of the 3-NPA²⁻ ligand in **1** and **2** (Figure 1 and Figure 4).

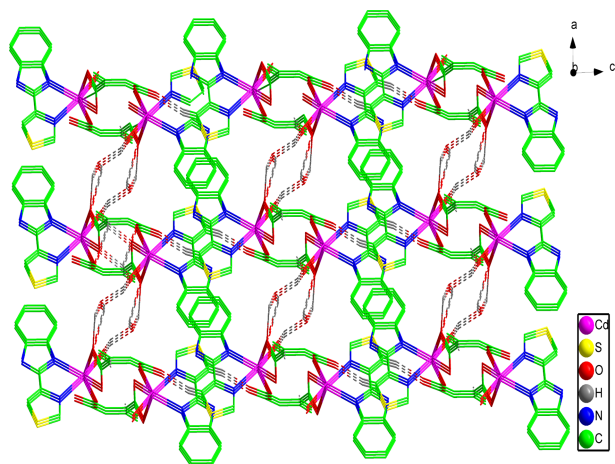


Figure 3. The 3D supramolecular structure of complex **1** via H-bonding. Unnecessary atoms are omitted for clarity.

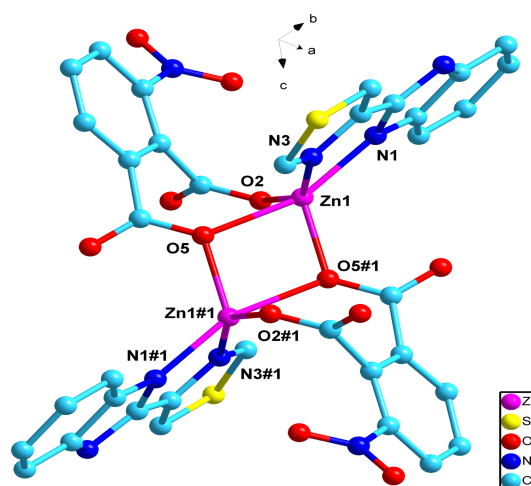


Figure 4. The coordination environment of Zn(II) ion of the complex **2**. All the hydrogen atoms are omitted for clarity. Symmetry codes: #1 = 1–*x*, 1–*y*, 2–*z*.

The carboxylate groups of the 3-NPA²⁻ ligand adopt μ 1- η^1 : η^0 and μ 2- η^2 : η^0 coordination modes (Figure S1b). No water molecules coordinated to the Zn atom in **2**. There is a different 4-membered ring consisting of deprotonated 3-nitrophthalic acid coordinated by two neighboring Zn atoms in **2**, as shown in Figure 4. The Zn(II) metal center in a distorted trigonal bipyramidal coordination sphere, which is defined by two oxygen donors (O2, O5#1) from two distinct 3-NPA²⁻ ligands and one nitrogen atom (N3) from a TBZ ligand in the equatorial positions while axial positions are furnished by two atoms (O5, N1) from one carboxylate group and a TBZ ligand, respectively. The average Zn–O and Zn–N distances are 2.041(5) and 2.097(2) Å. The C–H \cdots O hydrogen bonding plays an important role in stabilizing the crystal structure (Table S3). Two adjacent TBZ molecules are connected by π - π stacking interactions with a distance of 3.786(1) Å. The binuclear clusters are further extended by π - π stacking interactions and C–H \cdots O hydrogen-bonding into a 2D supramolecular framework (Figure S2).

The asymmetric unit of **3** shows that the Zn1 adopts a tetrahedral geometry, while Zn2 adopts a distorted trigonal bipyramidal geometry with two oxygen atoms (O7, O8) and a nitrogen atom (N4) of one TBZ located in the basal sites and the other two atoms (O1#1, N3) taken on the apical positions. The distances of O and Zn1 range from 1.924(3) to 1.984(3) Å and the Zn1–N bond length is 1.989(3) Å, both are somewhat longer to those seen in **1** and **2**, which is consistent with the fact that bond lengths in a tetrahedral geometry are generally shorter than those in other geometries. As depicted in Figure 5(a), each fully deprotonated 3-NPA²⁻ anion acts as μ 3-bridge linking three Zn centers via one unidentate carboxylate group and one bidentate carboxylate group (Figure S1c). In addition, it should be noted that TBZ spacers establish physical bridge between Zn atoms with Zn \cdots Zn separations of 5.928(2) Å, resulting in the formation of one-dimensional infinite double-chain (Figure 5(b)). The 1D chain is further linked by the weak O–H \cdots O

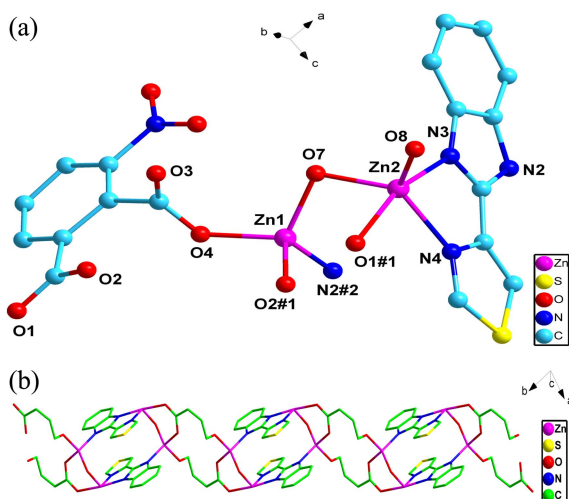


Figure 5. (a) The coordination environment of Zn(II) ion of the complex **3**. All the hydrogen atoms are omitted for clarity. Symmetry codes: #1 = 1-x, 2-y, 1-z; #2 = 2-x, 1-y, 1-z. (b) One-dimensional infinite double-chain of **3**. Unnecessary atoms are omitted for clarity.

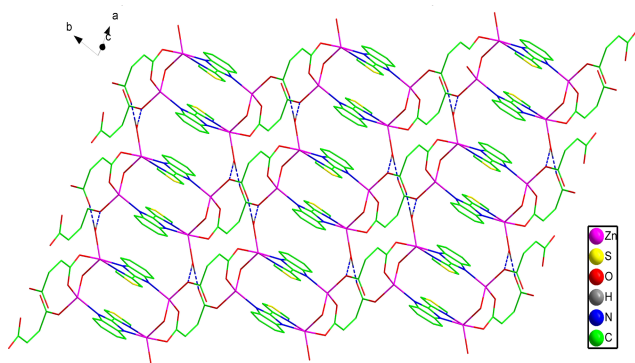


Figure 6. Infinite 2D networks of **3** connected by O-H...O hydrogen bonds (blue dashed line). Unnecessary atoms are omitted for clarity.

hydrogen bonds [O8-H8A...O3 = 2.678(5), O8-H8B...O4 = 2.736(4)], thus giving rise to the formation of a 2D sheet framework (Figure 6). Furthermore, these 2D sheets are connected by the weak nonclassical hydrogen bonds [C18-H18...O5 = 2.383(4)] to form a 3D supramolecular framework (Figure 7).

As shown in Figure 9, the asymmetric unit of **4** is composed of one Co center, one 3-NPA²⁻ anion, one TBZ ligand, and one coordinated water molecule. The Co center is six-coordinated to form octahedral geometry by O5, O6#1, and O7#2 from three distinct 3-NPA²⁻ ligands, N3 and N4 from the TBZ ligand, and O1 from one coordinated water molecule. The equatorial positions are occupied by the O1, O6#1, N3 and N4 atoms and the axial positions are occupied by the O5 and O7#2 atoms. The range of CoO bond lengths fall in 2.075(2)–2.381(2) Å and Zn-N distances are 2.095(2) and 2.149(2) Å, and all in the reasonable range.¹⁸ As the carboxylate groups adopt $\mu_1\text{-}\eta^1\text{:}\eta^0$ and $\mu_2\text{-}\eta^1\text{:}\eta^1$ modes (Figure S1c), each fully deprotonated 3-NPA²⁻ ligand acts as a linker to bridge three Co centers. The combination of the

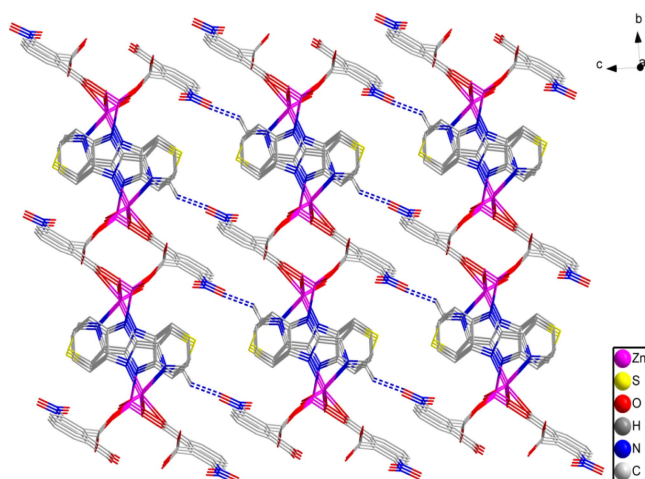


Figure 7. View of the 3D supramolecular structure of **3** showing hydrogen bonds (in blue dotted lines).

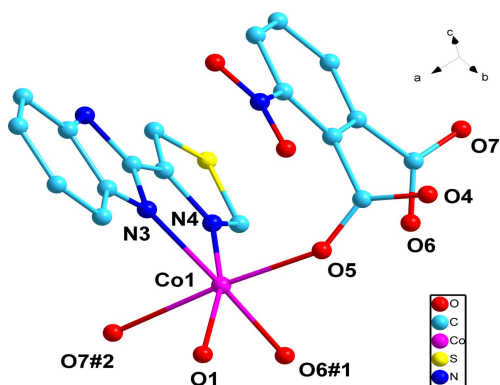


Figure 8. View of the coordination environment of the Co center in **4**. All the hydrogen atoms are omitted for clarity. Symmetry codes: #1 = -x, 2-y, -z; #2 = 1+x, y, z.

phenyl ring and the setwisted carboxylate groups result in the formation of one-dimensional infinite ladder-like chain (Figure 9). It is noteworthy that the weaker nonclassical hydrogen bonds were observed between C-H moieties and the uncoordinated oxygen atom (O3, O4), with the distances are 2.397(3) and 2.573(2) Å, thus these chains are further connected by hydrogen bonds to produce a 2D network structure (Figure 10(a)). Moreover, such layers are further united together through hydrogen bonds to present a 3D supramolecular structure (Figure 10(b)). It is no doubt for these weaker nonclassical hydrogen bonding interactions to contribute significantly to the alignment of the molecules in the crystalline state.

Comparison of the Structures. It is known that multicarboxylate ligands have been proved to be excellent structural constructors due to their various coordination modes.¹⁹ The different structures of the complexes **1-4** with transition metals and the same N-donor ancillary coligand, indicate that the multicarboxylate ligand have great influence on the structures of the complexes due to their different coordination modes. Therefore, comparison and comprehension of the coordination modes of the carboxylate ligand are a good

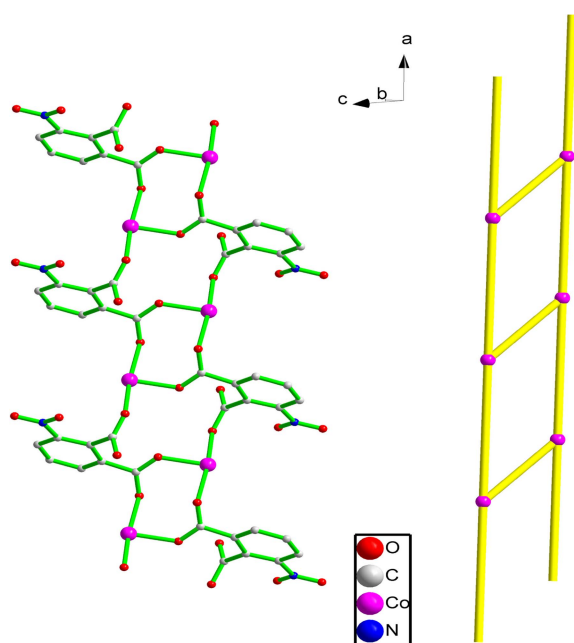


Figure 9. View of one-dimensional infinite ladder-like chain in **4**.

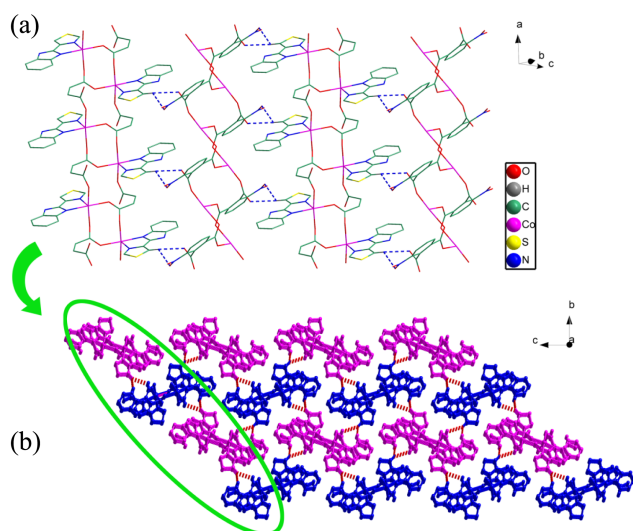


Figure 10. (a) Infinite 2D networks of **4** connected by C-H...O hydrogen bonds (blue dashed line). Unnecessary atoms are omitted for clarity. (b) View of the 3D structure of complex **4** via H-bonding (red dashed line). Unnecessary atoms are omitted for clarity.

and feasible method to predesign the coordination complexes. There are three kinds of coordination modes of 3-NPA²⁻ in the complexes **1-4** described above (Figure S1). In **3** and **4**, each 3-NPA²⁻ ligand adopts a μ_3 -bridging mode using its two carboxylate groups with μ_2 - η^1 : η^1 and μ_1 - η^1 : η^0 bis-chelating mode (Figure S1c) to form 1D chain polymers. In complexes **1** and **2**, 3-NPA²⁻ ligands exhibit different coordination modes as that in compounds **3** and **4**, the two carboxyl groups in **1** adopt μ_1 - η^1 : η^0 and μ_1 - η^1 : η^1 coordination modes, and the carboxyl groups coordinates with Zn(II) ions with μ_1 - η^1 : η^0 and μ_2 - η^2 : η^0 coordination modes in **2**, so two types of 0D molecular rings are obtained in **1** and **2**. In brief,

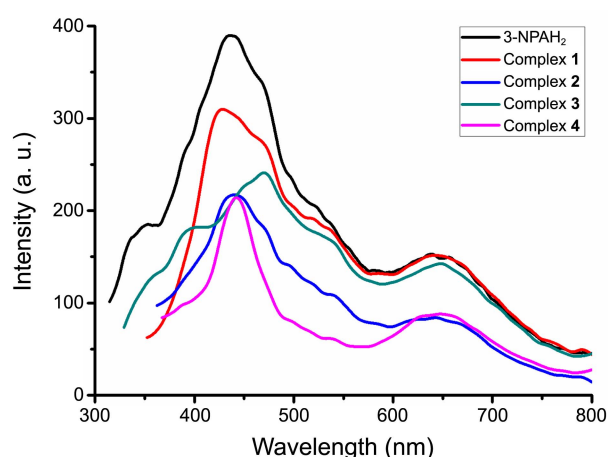


Figure 11. Emission spectra of free 3-NPAH₂ ligand and **1-4** in the solid state at room temperature.

the different coordination modes of the carboxylate groups lead to the formation of the coordination complexes with varied structures. In addition, the weak O-H...O hydrogen bonds and C-H...O nonclassical hydrogen bonds as well as π - π stacking also play important roles in affecting the final structures where complexes **1**, **3** and **4** have 3D supramolecular architectures, while complex **2** has a 2D supramolecular network.

IR Spectrum. In the IR spectra of the complexes **1**, **2** and **3**, the strong and broad bands at about 3500-3000 cm⁻¹ region are attributed to the symmetric O-H stretching modes and O-H bending modes, respectively. $\nu_{as}COO$ appears strong peaks at 1652 and 1587 cm⁻¹ in complex **1**, 1641 and 1601 cm⁻¹ in **2**, 1650 and 1634 cm⁻¹ in **3**, 1557 and 1540 cm⁻¹ in **4**. ν_sCOO appears peaks at 1457 and 1396 cm⁻¹ in **1**, 1454 and 1415 cm⁻¹ in **2**, 1457 and 1394 cm⁻¹ in **3**, 1456 and 1385 cm⁻¹ in **4**. For complexes **1-4**, the strong peak at 1556, 1557, 1557 and 1526 cm⁻¹ is attributed for $\nu_{as}NO_2$, the peaks at 1354, 1373, 1338 and 1376 cm⁻¹ are attributed for ν_sNO_2 , peaks at 1539, 1542, 1540 and 1506 cm⁻¹ is consistent with C=N, respectively. The C-S stretching band at about 1330 cm⁻¹ is observed in all complexes.

Fluorescence Properties. Luminescent complexes are of great interest due to their various applications in chemical sensors, photochemistry, and light-emitting diodes (LEDs).^{20, 21} Complexes **1-4** are insoluble in common organic solvents; hence photoluminescence properties of **1-4** and free 3-NPAH₂ ligand were investigated in the solid state at room temperature. As shown in Figure 11, the free 3-NPAH₂ ligand emits strong fluorescence centered at 438 nm (λ_{ex} = 233 nm). The luminescent behavior of free ligand arises from the π^* - π transitions of the aromatic rings.²² For the complexes, the emission bands are 429 nm (λ_{ex} = 236 nm) for **1**, 441 nm (λ_{ex} = 266 nm) for **2**, 469 nm (λ_{ex} = 239 nm) for **3**, 445 nm (λ_{ex} = 263 nm) for **4**, respectively. The emissions of complexes **1-4** may be a mixture of characters of intraligand and ligand-to-ligand charge transition (LLCT), and the observed red or a little blue shift of the emission maximum between the compounds and the ligands was considered to mainly

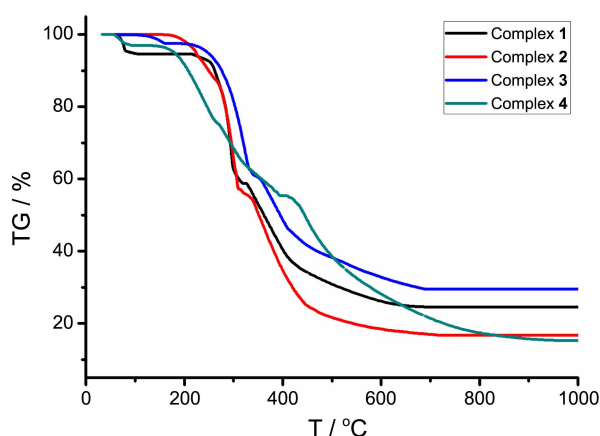


Figure 12. TG curves for complexes 1-4.

originate from the influence of the coordination of the ligand to metal atom.²³ The different locations and profiles of their emission/excitation peaks of complexes 1-4 may result from different metal centers and ligand chelation to the metal center, which may affect the rigidity of the whole network and further the energy transfer involved in the luminescence.²⁴

Thermogravimetric (TG) Analyses. Complexes 1-4 are air stable and can retain their structural integrity at room temperature for a considerable length of time; thus, TGA was conducted to determine the thermal stability of these crystalline materials, and the TG curves are shown in Figure 12. The TG curve of 1 shows the first loss of 5.37% in the temperature range of 61-102 °C, which indicates the exclusion of water molecules and coordinated water molecules (calcd, 6.46%); The second stage occurs between 217 and 317 °C, the anhydrous complex loses 35.85% of total weight, which is due to the decomposition of two 3-NPA²⁻ (calcd, 37.49%). The final weight loss of 34.22% (calcd, 35.90%) corresponds to the loss of two TBZ in the temperature range of 330-704 °C. The remaining residue corresponds to the formation of CdO (obsd, 24.55%; calcd, 23.02%).

For complex 2, the first weight loss of 42.83% from 187 to 309 °C, corresponds to the loss of the 3-NPA²⁻ (calcd, 44.05%). The residuary TBZ section loses weight of 40.40% (calcd, 42.18%) subsequently from 315 to 719 °C. The residual percentage weight at the end of the decomposition of the complex is observed 16.77%, it corresponds to the ZnO (calcd, 17.14%).

For 3, the weight loss attributed to the gradual release of coordinated water molecules is observed in the range of 105-159 °C (obsd, 2.43%; calcd, 3.14%). When the temperature holds on rising, the product lost 34.90% of the total weight in the temperature range of 189 to 330 °C, which is related to the loss of 3-NPA²⁻ (calcd, 36.42%). Beyond 336 °C, the TBZ decomposes gradually, the products lose 33.17% of the total weight (calcd, 34.88%). Then the remaining weight is assigned to ZnO (obsd, 29.50%; calcd 28.35%).

The TGA curve of 4 shows three main weight losses. The first one occurs in the temperature range of 58-92 °C corresponding to the release of one coordinated water molecules per formula unit. The observed weight loss (3.01%) is in

agreement with the calculated one (3.71%). The dehydrated sample can be stable up to 171 °C, then the last two weight losses occur, indicating that the whole framework collapse because of the decomposition of the 3-NPA²⁻ (found, 41.63%; calcd, 43.00%) and TBZ (obsd, 40.08%; calcd, 41.18%).

Conclusion

In summary, four novel transition-metal coordination complexes have been synthesized by employing the 3-NPAH₂ as the main ligand and TBZ as auxiliary ligand under hydrothermal conditions. In complexes 14, the carboxylic groups exhibit different coordination modes and coordination capacity, and connect the metal ions into different metal-carboxylates subunits with 0D dinuclear units and 1D chain structures, which show a great effect on the formation of the final architectures. The weak O-H...O hydrogen bonds and C-H...O nonclassical hydrogen bonds as well as weak nonclassical hydrogen bonds and π - π stacking also play important roles in affecting the final structure. The present different structures of complexes 1-4 are extended into 2D or 3D supramolecular frameworks *via* the hydrogen bonding and the π - π stacking interactions. In addition, the fluorescent properties for the complexes prove that complex 1 may be good candidates for potential applications in fluorescent. Also, thermal decomposition process of the complexes was investigated.

Acknowledgments. The authors thank the National Natural Science Foundation of China (20761002), PR China, the Natural Science Foundation of Guangxi (053020), P.R. China and Guangxi University for Nationalities. And the publication cost of this paper was supported by the Korean Chemical Society.

References

- (a) Perry, J. J. IV.; Perman, J. A.; Zaworotko, M. J. *Chem. Soc. Rev.* **2009**, 38, 1400. (b) Wang, Z.; Cohen, S. M. *Chem. Soc. Rev.* **2009**, 38, 1315. (c) Dueren, T.; Bae, Y. S.; Snurr, R. Q. *Chem. Soc. Rev.* **2009**, 38, 1237. (d) Ma, L.; Abney, C.; Lin, W. *Chem. Soc. Rev.* **2009**, 38, 1248. (e) Farha, O. K.; Hupp, J. T. *Acc. Chem. Res.* **2010**, 43, 1166. (f) Ferey, G.; Serre, C. *Chem. Soc. Rev.* **2009**, 38, 1380.
- (a) Murray, L. J.; Dinca, M.; Long, J. R. *Chem. Soc. Rev.* **2009**, 38, 1294. (b) Shimizu, G. K. H.; Vaidyanathan, R.; Taylor, J. M. *Chem. Soc. Rev.* **2009**, 38, 1430. (c) Chen, B.; Xiang, S. C.; Qian, G. *Acc. Chem. Res.* **2010**, 43, 1115. (d) Pan, M.; Lin, S. M.; Li, G. B.; Su, C. Y. *Coord. Chem. Rev.* **2011**, 255, 1921. (e) Qiu, S. L.; Zhu, G. S. *Coord. Chem. Rev.* **2009**, 253, 2891.
- Forster, P. M.; Stock, N.; Cheetham, A. K. *Angew. Chem. Int. Ed.* **2005**, 44, 7608.
- Zhou, Y. F.; Lou, B. Y.; Yuan, D. Q.; Xu, Y. Q.; Jiang, F. L.; Hong, M. H. *Inorg. Chim. Acta* **2005**, 358, 3057.
- Chen, S. M.; Lu, C. Z.; Zhang, Q. Z.; Liu, J. H.; Wu, X. Y. *Eur. J. Inorg. Chem.* **2005**, 423.
- (a) Lin, W.; Rieter, W. J.; Taylor, K. M. L. *Angew. Chem.* **2009**, 121, 660. (b) Jiang, H. L.; Xu, Q. *Chem. Commun.* **2011**, 47, 3351. (c) Caskey, S. R.; Wong-Foy, A. G.; Matzger, A. J. *J. Am. Chem. Soc.* **2008**, 130, 10870. (d) Morris, R. E.; Wheatley, P. S. *Angew. Chem.* **2008**, 120, 5044.

7. (a) White, K. A.; Chengelis, D. A.; Gogick, K. A.; Stehman, J.; Rosi, N. L.; Petoud, S. *J. Am. Chem. Soc.* **2009**, *131*, 18069. (b) Law, G. L.; Wong, K. L.; Tam, H. L.; Cheah, K. W.; Wong, W. T. *Inorg. Chem.* **2009**, *48*, 10492. (c) Lewis, D. J.; Glover, P. B.; Solomons, M. C.; Pikramenou, Z. *J. Am. Chem. Soc.* **2011**, *133*, 1033.
 8. Brammer, L. *Chem. Soc. Rev.* **2004**, *33*, 476.
 9. Seide, S. R.; Stang, P. J. *Acc. Chem. Res.* **2002**, *35*, 972.
 10. Caulder, D. L.; Raymond, K. N. *Acc. Chem. Res.* **1999**, *32*, 975.
 11. Lu, X. L.; Wu, H.; Ma, J. F.; Yang, J. *Polyhedron.* **2011**, *30*, 1579.
 12. (a) Lin, X.; Telepeni, I.; Blake, A. J.; Dailly, A.; Brown, C. M.; Simmons, J. M.; Zoppi, M.; Walker, G. S.; Thomas, K. M.; Mays, T. J.; Hubberstey, P.; Champness, N. R.; Schroder, M. *J. Am. Chem. Soc.* **2009**, *131*, 2159. (b) Zhang, X. T.; Fan, L. M.; Sun, Z.; Zhang, W.; Li, D. C.; Dou, J. M.; Han, L. *Cryst. Growth Des.* **2013**, *13*, 792. (c) Choi, H. S.; Suh, M. P. *Angew. Chem.* **2009**, *48*, 6865.
 13. (a) Guo, F.; Wang, F.; Yang, H.; Zhang, X. L.; Zhang, J. *Inorg. Chem.* **2012**, *51*, 9677. (b) Tsai, H. L.; Yang, C. I.; Wernsdorfer, W.; Huang, S. H.; Jhan, S. Y.; Liu, M. H.; Lee, G. H. *Inorg. Chem.* **2012**, *51*, 13171. (c) Lim, J. M.; Kim, P.; Yoon, M. C.; Sung, J.; Dehm, V.; Chen, Z. J.; Wurthner, F.; Kim, D. *Chem. Sci.* **2013**, *4*, 388.
 14. (a) Dai, F.; Dou, J.; He, H.; Zhao, X.; Sun, D. *Inorg. Chem.* **2010**, *49*, 4117. (b) Guo, Z.; Cao, R.; Wang, X.; Li, H.; Yuan, W.; Wang, G.; Wu, H.; Li, J. *J. Am. Chem. Soc.* **2009**, *131*, 6894. (c) Liu, T. F.; Lu, J.; Guo, Z.; Proserpio, D. M.; Cao, R. *Cryst. Growth Des.* **2010**, *10*, 1489.
 15. Higashi, T. *Program for Absorption Correction*; Rigaku Corporation: Tokyo, Japan, 1995.
 16. Sheldrick, G. M. *SHELXTL V5.1 software reference manual*. Bruker AXS, Inc. Madison, Wisconsin, USA, 1997.
 17. Dai, J. C.; Wu, X. T.; Fu, Z. Y.; Cui, C. P.; Hu, S. M.; Du, W. X.; Wu, L. M.; Zhang, H. H.; Sun, R. Q. *Inorg. Chem.* **2002**, *41*, 1391.
 18. Zang, S.-Q.; Su, Y.; Li, Y.-Z.; Ni, Z.-P.; Zhu, H. Z.; Meng, Q.-J. *Inorg. Chem.* **2006**, *45*, 3855.
 19. (a) Hijikata, Y.; Horike, S.; Tanaka, D.; Groll, J.; Mizuno, M.; Kim, J.; Takata, M.; Kitagawa, S. *Chem. Commun.* **2011**, *47*, 7632. (b) Mihalcea, I.; Henry, N.; Clavier, N.; Dacheux, N.; Loiseau, T. *Inorg. Chem.* **2011**, *50*, 6243. (c) Lama, P.; Sanudo, E. C.; Bharadwaj, P. K. *Dalton Trans.* **2012**, *41*, 2979. (d) Luebke, R.; Eubank, J. F.; Cairns, A. J.; Belmabkhout, Y.; Wojtas, L.; Eddaoudi, M. *Chem. Commun.* **2012**, *48*, 1455.
 20. Cui, Y.; Yue, Y.; Qian, G.; Chen, B. *Chem. Rev.* **2012**, *112*, 1126.
 21. (a) Li, X.; Sun, H. L.; Wu, X. S.; Qiu, X.; Du, M. *Inorg. Chem.* **2010**, *49*, 1865. (b) Hu, J. S.; Shang, Y. J.; Yao, X. Q.; Qin, L.; Li, Y. Z.; Guo, Z. J.; Zheng, H. G.; Xue, Z. L. *Cryst. Growth Des.* **2010**, *10*, 2676.
 22. Zang, S.-Q.; Dong, M.-M.; Fan, Y.-J.; Hou, H.-W.; Mak, T. C. W. *Cryst. Growth Des.* **2012**, *12*, 1239.
 23. (a) Chang, Z.; Zhang, A. S.; Hu, T. L.; Bu, X. H. *Cryst. Growth Des.* **2009**, *9*, 4840. (b) Guo, J.; Ma, J. F.; Liu, B.; Kan, W. Q.; Yang, J. *Cryst. Growth Des.* **2011**, *11*, 3609.
 24. (a) Wang, S. N.; Xing, H.; Li, Y. Z.; Bai, J. F.; Pan, Y.; Scheer, M.; You, X. Z. *Eur. J. Inorg. Chem.* **2006**, 3041. (b) Yao, X.-Q.; Cao, D.-P.; Hu, J.-S.; Li, Y.-Z.; Guo, Z.-J.; Zheng, H.-G. *Cryst. Growth Des.* **2011**, *11*, 231.
-